

# Performance Evaluation of IRI-Plas 2017 model with Ionosonde Data Measurements of Ionospheric Parameters

Endeshaw Lake (✉ [endesowlake@gmail.com](mailto:endesowlake@gmail.com))

university <https://orcid.org/0000-0002-6400-9448>

Alene Seyoum

ESSTI: Ethiopian Space Science and Technology Institute

---

Full paper

**Keywords:** IRI-Plas model, Ionosonde, Electron density, NmF2, hmF2, foF2

**Posted Date:** January 17th, 2022

**DOI:** <https://doi.org/10.21203/rs.3.rs-1233167/v1>

**License:**   This work is licensed under a Creative Commons Attribution 4.0 International License.

[Read Full License](#)

---

# Abstract

This study presents the performance evaluation of International Reference Ionosphere extended to the plasmasphere (IRI-Plas 2017) model from the Addis Ababa ionosonde station, Ethiopia ionospheric parameters measurement with geographic latitude  $9.00^{\circ}$  N and longitude  $38.70^{\circ}$  E; geomagnetic latitude  $0.16$ , geomagnetic longitude  $110.44$ ) in selected days of the year 2014. During comparison, hourly and day-to-day variability of ionospheric parameters of the electron density profile, peak electron density (NmF2), peak height (hmF2) and critical frequency (foF2) measurements are considered. In the evaluation of the IRI-Plas 2017 model with the ionosonde data, the percentage deviation and the correlation coefficient (R) is used as the measure of the performance of the IRI-Plas 2017 model. The overall results, show that the IRI-Plas 2017 model mostly overestimates in most altitudes and hours of electron density measurements. The IRI-Plas 2017 model has a good agreement with the ionosonde electron density measurement from 100 km to 200 km altitude and mostly during in between 0:00-06:00 UT and 12:00-18:00 UT hours, while the model biases in other altitudes and hours with overestimate or underestimate in the ionosonde electron density measurements. The IRI-Plas 2017 model has a good correlation during after midnight and around midday hours with about  $\pm 2$  percentage deviation from the ionosonde electron density measurement. The model has high percentage deviation value of electron density measurements mostly in between altitudes from 200 km to 450 km and during early nighttime and before midnight hours. The IRI-Plas 2017 model measurements of the NmF2, hmF2 and foF2 mostly underestimates from the ionosonde data during the night-time (18:00 UT- 06:00 UT) and overestimates during day-time (06:00 UT-18:00 UT). The IRI-Plas 2017 model measurement of the foF2 values are in a good agreement with the ionosonde result than in hmF2 and NmF2 and the model measurement of the NmF2 values are closer than hmF2.

## 1. Introduction

The ionosphere is the fundamental area of space weather with its notably variable structure in both area and time. The topside electron density is the most significant for all empirical ionospheric models. Nowadays, the profile-based empirical ionospheric models are required for the trans-ionospheric radiowaves propagation duties, navigation and communication. The ionospheric parameters, such as total electron content (TEC), electron density profile (Ne), maximum electron density (NmF2), maximum ionization top of ionospheric layers (hmF2), critical layer frequency (foF2), electron and ion temperatures are modeled in different models. The electron density profiles and TEC computation results of IRI-Plas across the European region are reviewed in depth (Maltseva et al. 2013; Zakharenkova et al. 2015) and an equivalent evaluation is performed for the Indian region (Panda et al. 2015). The IRI-Plas model is likewise in comparison with different ionospheric models (Okoh et al. 2018; Maltseva et al. 2015; Cherniak and Zakharenkova 2016). Despite the fact, that there were a few inconsistencies with the ionosonde data in all of the above-mentioned investigations, IRI-Plas is a highly powerful model in describing the ionosphere in different locations during storm and quiet times.

The International Reference Ionosphere (IRI) model is an empirical, deterministic and climatic model of the ionosphere up to 2000 km in peak. Currently, IRI extended to Plasmasphere (IRI-Plas) model has been evolved to extend the hobby region of IRI to the GPS orbital altitude of 20,000 km. The IRI and IRI-Plas models offer ionospheric parameters such as total electron content, electron density profile, peak electron density ( $NmF2$ ), peak height ( $hmF2$ ), critical frequency ( $foF2$ ), electron and ion temperatures in line with their height profiles. In order to update the model to contemporary ionospheric situations, IRI-Plas can input F2 layer critical frequency ( $foF2$ ), maximum ionization height ( $hmF2$ ) and total electron content (TEC). The online IRI-Plas 2017 model has been developed to allow the ionospheric community to execute many activities at different places, dates and times with an option of the  $foF2$ ,  $hmF2$  and TEC inputs in a single user approach. The solar activity option is selected as sun spot number (SSN); the F-peak model is selected as CCIR (international Radio Consultative Committee) and the  $foF2$  storm model option also can be chosen as 'on' (Sezen et al. 2018).

Currently, numerous studies made a number of detailed comparison of measured ionospheric parameters with the IRI-Plas model. Maltseva et al. (2015) probed the effectiveness of the International Reference Ionosphere extended to Plasmasphere model (IRI-Plas) and the Neustreliz Global Model (NGM) in estimating VTEC in varied locations. They concluded that VTEC-NGM and VTEC-IRI-Plas generated better results than VTEC-IRI at middle and high latitudes, and that the IRI-Plas model predicts better than NGM during the winter months. Zakharenkova et al. (2015) compared the mid-latitude GPS station TEC statistics to the IRI-2012 and IRI-Plas models TEC data. As a response, they concluded that the IRI-Plas model overestimated TEC values, specially during low and medium solar activity years. Arikan et al. (2015) reviewed the performance of IRI-Plas model maps through evaluating it with the Global Ionospheric Maps (GIM) on a magnetically disturbed days. As a result of the study, they found that the global distribution value of TEC was different due to the effects of geomagnetic disturbances. Adebiji et al. (2016) studied the diurnal and seasonal behavior of GPS-TEC for the year 2014 over 8 stations located inside the Southern African equatorial and low-latitude regions and made a comparison with the outcomes of the data derived from the IRI-2012 and IRI-Plas models. Their assessment tested that diurnal and seasonal structures of modeled TEC follow pretty properly with the observed TEC in all stations and on the same time the prediction errors exhibit latitudinal variations and seasonal trends. Cherniak et al. (2016) analyzed the modeling accuracy of NeQuick2 and IRI-Plas models during intervals of quiet and medium solar activity on a global scale. Zhang et al. (2017) handled a comparison study with the IRI-Plas model by using Topside Ionospheric and Plasmaspheric Electron content (TPEC) data records obtained from the podTEC measurements of the Precise Orbit Determination (POD) antenna on board the COSMIC Low Earth Orbit (LEO) satellites monitoring GPS signals. Alçay et al. (2017) evaluated the TEC estimate performance of the IRI-2012 and IRI-Plas models in different parts of the world and they found a strong agreement between GPS-TEC and models TEC on quiet days. Sezen et al (2018) studied the IRI-Plas model and offer some comparisons between IRI-Plas outputs and ionosonde measurements and they concluded that the model values are closer to ionosonde results in  $foF2$  than in  $hmF2$ . In a study by Okoh et al. (2018), TEC obtained from the NeQuick and the IRI-Plas models are compared with the GPS-TEC acquired from a single station and they have been observed that IRI-Plas model, without an external input

overestimate GPS-TEC particularly for the duration of local daytime. Ezquer et al. (2018) compared the TEC estimations of the NeQuick 2 and IRI-Plas models to GPS-derived TEC values over a low-latitude and South American area and they found that, at low latitudes, IRI-Plas model had higher predictions, on the other hand, at high latitudes, NeQuick model made higher predictions. Gordiyenko et al. (2018) have been shown that the seasonal variations of the F-layer peak electron density (NmF2) measured at the Alma-Ata and total electron content (TEC) values derived from the Global Ionospheric Maps (GIM) for the Alma-Ata region have different trends. Additionally, they concluded that the daytime NmF2 values are more in winter than in summer time, however the day-time GIM-TEC has more values in the summer time as compared to those in winter season. Gordiyenko et al. (2019) made a comparison between IRI-Plas foF2 model and ionosonde foF2 measurement and they found that the IRI-Plas foF2 model are in a good agreement with the ionosonde showing comparable structures, similar magnitudes reflecting the winter anomaly within the diurnal variations. They concluded that the IRI-Plas model shows a significant overestimation of the daylight hours GIM-TEC values for winter conditions in any respect locations of Russian and Kazakhstan regions and during summer month, the IRI-Plas model demonstrates different results showing a scientific underestimation or overestimation in high or low solar activity.

Since IRI-model provides the ionospheric parameters as much as 2000 km, it will not longer correctly predict the the ionospheric parameters up to GPS satellites located in altitude of 20,200 km. It is critical to extrapolate the ionosphere as much as the GPS satellite height of the IRI-model to overcome this situation (Alçay et al. 2017). The IRI-Plas model provides many ionospheric parameters with an internet interface presented with the aid of the IOBOLAB group at [www.ionolab.org](http://www.ionolab.org). The total electron content (TEC), electron density profile (Ne), peak electron density (NmF2), peak height (hmF2), critical frequency (foF2) are important parameters for the study of the ionosphere. The IRI-Plas 2017 model has measured these important ionospheric parameters directly from it's homepage.

In this study, we're going to present the performance evaluation of the IRI-Plas model of version 2017 with Addis Ababa ionosonde station ionospheric parameters measurement of the electron density profile (Ne), peak electron density (NmF2), peak height (hmF2) and critical frequency (foF2). Among the regions of the ionosphere, the ionospheric F region has the highest electron density and as a result influences HF radio waves within the most significant way. The ionospheric parameters at the F layer has been always a special interest for experimentally and in the theoretical modeling of the ionosphere formation (Kutiev et al. 2013; Seyoum et al. 2019). The ionospheric parameters at the F region has been traditionally studied through ionosonde observations (Davies 1990; Hunsucker 1991; Rawer 2013). The performance the IRI-Plas model is not tested in a passable way in different areas of the world. Hence, it is important to study the performance and capability of the latest version of the IRI-Plas 2017 model with the ionosonde ionospheric parameters over Ethiopian region.

## 2. Methodology And Data

An ionosonde is a high frequency (HF) radar used for ionospheric observations and probing. The ionosonde emits rapid radio energy pulses vertically into the ionosphere. These pulses are reflected back

in the direction of the ground and the ionosonde records the time delay between transmission and reception of pulses as a measurement of the ionospheric reflection height. Ionosonde recordings are usually displayed graphically, as virtual height towards band of frequency, which is known as ionogram. From an ionogram, essentially it's miles viable to measure the critical frequencies of every layer, the virtual heights and additionally the electronic density profile can be derived as characteristic of the height. In addition to this type of ionospheric parameters measurement ionospheric models are very important. Among these ionospheric models the one that measure ionospheric parameters is International Reference Ionosphere extended to Plasmasphere (IRI-Plas). The IRI-Plas model gives different geomagnetic and solar proxy values to present the ionospheric variability. The output of on-line IRI-Plas is supplied as a textual content report that may be copied or downloaded for further processing with a favored software tool. The three required inputs are user described location, date and time. The online useful resource for IRI-Plas 2017 model version can be found at web of the IONOLAB Ionospheric Research Laboratory, Turkey <http://ionolab.org>.

## **2.1 Ionospheric Parameters Measurement from Ionosonde**

The ionosonde is an instrument that measures ionization in the ionosphere and a very well established instrument. Due to its relative low cost of installation and operations, a massive variety of these devices are spread around the world to continuously screen the ionosphere (Hargreaves 1992). The ionosonde data that is important to compute the relationship between electron density profile, foF2, NmF2 and hmF2 are obtained from Addis Ababa ionosonde station geographic latitude 9.00° N and longitude 38.70° E; geomagnetic latitude 0.16, geomagnetic longitude 110.44) in selected days of the year 2014. The ionosonde is connected to a computer that is used to gather, store and process ionograms in a digital form. The ionosonde provides virtual reflection height data as a function of sign frequency. The data used for the present study are ionospheric parameters of the electron density profile, peak electron density (NmF2), peak height (hmF2) and critical frequency (foF2) deduced from the ionograms and true height inversions (Titheridge 1985; Reinisch and Huang 2001). The ionosonde data availability from Addis Ababa station is quite limited and suffers from missing values. Therefore, in this study only three months of days (May, June and July) with non missing data values are considered.

## **2.2 Ionospheric Parameters Measurement from IRI-Plas 2017 model**

The international standardization organization recently, advocated the IRI model for the specification of ionosphere plasma densities and temperatures and indexed several plasmasphere models for extending IRI to plasmaspheric altitudes. One of the empirical models that may offer ionospheric characteristics up to GPS satellite orbital height of 20,200 km is International Ionosphere Extended to Plasmasphere (IRI-Plas) model. The IRI-Plas model has been offered as a possible model for the IRI model's plasmasphere extension (Gulyaeva and Bilitza 2012; Gulyaeva et al. 2002a, b, 2013; Endeshaw 2020). In this study, electron density profile, peak electron density (NmF2), peak height (hmF2) and critical frequency (foF2) values obtained from the IRI-Plas model are compared with ionosonde measurements. For the user defined location, date and time offered at Online IRI-Plas service of IONOLAB group is available at

www.ionolab.org ( Sezen et al., 2013; 2018). In this study the default option of the model is used for solar activity and geomagnetic index values.

In the comparison of the IRI-Plas 2017 model data with the ionosonde data measurement, it is essential to communicate the accuracy of the model measurement to understand how much error is associated with the ionosonde data. The comparison of the measurement value by finding out how much the model deviate from the ionosonde data and this expression is known as percent error or percent deviation. The percent deviation (% dev) between the IRI-Plas 2017 model and ionosonde ionospheric parameters data have been determined by using the following equation:

$$\% \text{ div} = \left( \frac{\text{IonosphereParameters} - \text{IRIPlasParameters}}{\text{IonosphereParameters}} \right) \times 100 \quad (1)$$

where, % div, IonosphereParameters, IRI PlasParameters represents the percent deviation, ionospheric parameters value for ionosonde and IRI-Plas 2017 model respectively.

Additionally, to evaluate the statistical measurement of the strength of the relationship between the values of the data ionosonde and IRI-Plas 2017 model, the correlation coefficient is used as the measure of the performance of the model. The Pearson correlation coefficient (R) between the ionosonde and IRI-Plas 2017 model is given by the formula:

$$R = \frac{n(\sum MI) - (\sum I)(\sum M)}{\sqrt{(n \sum I^2 - (\sum I)^2)(n \sum M^2 - (\sum M)^2)}} \quad (2)$$

Where, R- correlation coefficient, n- number of data, I - ionospheric parameters of the ionosonde and M - ionospheric parameters of the IRI-Plas 2017 model. The numerator is the co-variance and the denominator is the product of the standard deviation between the data of the ionosonde and IRI-Plas 2017 model.

### 3. Results And Discussion

The Earth's ionosphere is a highly dynamic plasma medium that continues to attract the interest of researchers and practitioners. Among these Earth's ionosphere parameters electron density profile, peak electron density (NmF2), peak height (hmF2) and critical frequency (foF2) values obtained from the ionosonde and IRI-Plas model measurements are taken into consideration in this study. Electron density is calculated from the sum of the ion densities. As a result, electron density profiles (EDPs) serve as a valuable resource for researchers studying the structure and behavior of the ionosphere. From Figures 1-4 below the comparison of ionosonde and IRI-Plas 2017 model measurements of the electron density profiles (EDP) are presented on different days of the year 2014. As shown in Figure 1a-1t, the IRI-Plas 2017 model shows a good correlation in most hours as compared to ionosonde electron density measurement. The IRI-Plas 2017 model underestimates as shown in the Figure 1a, b, f, h and l and

overestimates from the ionosonde measurement in the Figure 1 c, d, e, g, h, i, j, k, m, o, p, q, r, s and t, but underestimates in some hours about above 400 km altitude in the Figure 1 c, e, i, o, p, q, r, s and t.

As shown in Figure 2, the plots b (06:00 UT), d (14:00 UT), h (15:00 UT), m (15:00 UT), p (3:00 UT) and r (16:00 UT) indicate that a good agreement in the ionosonde measurement with slightly less underestimate or overestimate. In plots of a, h, m and q the IRI-Plas 2017 model shows underestimation, while in the plots of c, f, i, k, l, o and t shows overestimation in different hours of the ionosonde electron density measurements. From Figure 3, the IRI-Plas 2017 model mostly overestimates in the plots of a, b, f, h, i, j, l, m and t and underestimates in the plots of n, o, p and s with the electron density measurements. The IRI-Plas 2017 model indicates the worst fit with the ionosonde electron density measurement in the plots of a, b, i, j, k, m and t and the model shows intermediate fit in the other plots of Figure 3. As shown in Figure 4, the model indicates that a good agreement in the ionosonde measurement in the plots of b, c, d, q, h, l and s; overestimates in the plot of a, e, i, k, l, n, r and t and underestimate in the plots of f, j, p and s in the electron density profile measurement. Generally the IRI-Plas 2017 model has a good agreement with the ionosonde electron density measurement from 100 km to 200 km altitude and mostly during in between 0:00 UT – 06:00 UT and 12:00 UT-18:00 UT hours, while the model biases in other altitudes and hours with slightly less or more overestimate or underestimate in the ionosonde electron density measurement as shown in Figures 1, 2, 3 and 4.

Figure 5 shows, the altitudinal percentage deviation of the IRI-Plas 2017 model in selected days with hourly variability of the electron density measurements. The deviation versus altitude bar graph indicates that the IRI-Plas 2017 model underestimate, overestimate and correlate in altitude and time. The percent deviation is the value of the difference divided by the observation value times 100. From the bar Figure, the positive percentage deviation indicates that underestimation of the IRI-Plas 2017 model from the ionosonde electron density measurements, while negative percentage deviation indicates overestimation of the IRI-Plas 2017 model from the ionosonde measurements.

As shown from Figure 5, the IRI-Plas 2017 model in most hours overestimate the electron density measurement as compared to ionosonde measurement in lower altitudes with slightly less percentage deviations. The maximum percentage deviation (overestimation with -21%) was indicated on June 08 2014, 19:00 UT, this may be due to the week geomagnetic storm (starting to June 08 2014 at 7:00 UT hour the Dst value decreases to -34 nT and attain the minimum value of -37 nT on June 08 2014 at 24:00 UT hour). In this study, we can't see the detailed measurement of the IRI-Plas 2017 model performance during other strong disturbed days due to the limited ionosonde data availability from Addis Ababa station. The researchers may see the IRI-Plas 2017 model performance on the disturbed times on other fully data available ionosonde stations. The model has a good correlation during after midnight (04:00 UT and 06:00 UT hours with around (-2.5 %, 0.5 %), (-2 %, 0.5 %) percentage deviation respectively) and during around midday hours (11:00 UT and 12:00 UT hours with around  $\pm 1$  percentage deviation). The model has high percentage deviation value of electron density measurements mostly in between altitudes from 200 km to 450 km and during early nighttime and before midnight hours with values -21% and 8% for overestimation and underestimation respectively. The IRI-Plas 2017 model overestimates totally

during June 17 2014 at 14:00 UT and mostly on June 09 2014 at 06:00 UT, June 19 2014 at 15:00 UT, June 18 2014 at 16:00 UT, July 28 2014 at 17:00 UT, June 05 2014 at 18:00 UT, June 08 2014 at 19:00 UT, June 18 2014 at 21:00 UT, June 13 2014 at 21:00 UT and June 20 2014 at 22:00 UT hours. The model underestimates mostly during days on June 07 2014 at 01:00 UT, May 30 2014 at 11:00 UT and May 30 2014 at 12:00 UT hours.

From Figures 6-12, the measurement of peak electron density (NmF2), peak height (hmF2) and critical frequency (foF2) (upper panel), percentage deviation from bar graph (middle panel) and correlation coefficient (R) from scatter plot (bottom panel) of the IRI-Plas 2017 model and ionosonde measurements are presented. The percentage deviation shows either overestimate or underestimate of the IRI-Plas 2017 model from the ionosonde measurements. The correlation coefficient shows a relationship between the IRI-Plas 2017 model and ionosonde measurements. The correlation coefficient (R) is a statistical measure of the magnitude and direction of the linear relationship between two measurements. A correlation of -1.0 implies that there is a perfect inverse correlation. A correlation value of 1.0 indicates that there is a perfect positive relationship. Values of 0.0 or close to zero indicate a weak or non-existent linear relationship. Linear regression analysis can be used to calculate the correlation coefficient.

As shown in Figure 6, the IRI-Plas model underestimates the NmF2 measurement in between from 20:00 UT to 03:00 UT hours with maximum deviation about 3% and overestimates mostly in between 05:00 UT and 20:00 UT hours with maximum deviation about -5%. From the scatter plot the correlation coefficient of the IRI-Plas model with the ionosonde measurement is (R= 0.45). From the hmF2 measurement of the IRI-Plas model underestimates in between from 18:00 UT to 05:00 UT hours with maximum deviation about 21% and overestimates mostly in between from 05:00 UT to 18:00 UT hours with maximum deviation about -41%. And the scatter plot of the hmF2 measurement correlation coefficient of the IRI-Plas model with the ionosonde measurement is (R= -0.16). The IRI-Plas model measurement of the critical frequency (foF2) shows a good agreement with the ionosonde measurement with maximum percentage deviations of 0.25% (underestimate) and -55% (overestimate) and the correlation coefficient is (R= 0.64).

As shown in Figures 7- 12, the IRI-Plas model underestimates the NmF2 measurement in between from 16:00 UT to 01:00 UT (Fig. 7), from 21:00 UT to 02:00 UT and partially in some hours (Fig. 8), from 23:00 UT to 05:00 UT with other fluctuations (Fig. 9), inconsistent fluctuation (Fig. 10), from 21:00 UT to 07:00 UT (Fig. 11) and from 20:00 UT to 02:00 UT (Fig. 12) hours with maximum deviation about 4%, 4%, 3%, 3% 3% and 3% respectively. And the model overestimates mostly in between from 05:00 UT to 20:00 UT hours in most Figures with maximum deviation about -7% (Fig. 9) as shown in Figures 7-12. From the scatter plots the correlation coefficient of the IRI-Plas model with the ionosonde measurements are R= 0.58, 0.46, 0.51, 0.64, 0.35 and 0.39 on June 09, 10, 11, 13, 14 and 15 2014 (Figs. 7-12) respectively.

From the hmF2 measurement, the IRI-Plas model underestimates mostly in between from 15:00 UT to 05:00 UT hours with maximum deviation about 40% and overestimates mostly in between from 05:00 UT to 15:00 UT hours with maximum deviation about -60% as shown in Figures 7-12. From the scatter plot of the hmF2 measurement correlation coefficient of the IRI-Plas model with the ionosonde measurements

are  $R = -0.49, -0.27, -0.06, 0.07, 0.11$  and  $-0.02$  on June 09, 10, 11, 13, 14 and 15 2014 (Figs. 7-12) respectively. The IRI-Plas model measurement of the critical frequency ( $f_oF_2$ ) shows a good agreement with the ionosonde measurement in most hours. The IRI-Plas model overestimates mostly in between from 07:00 UT to 15:00 UT (Figs. 7-12) with maximum percentage deviations  $-50\%$  and inconsistent fluctuation from other hours as shown in bar graphs (Figs. 7-12). From the scatter plots the correlation coefficient of the IRI-Plas model with the ionosonde critical frequency ( $f_oF_2$ ) measurements are  $R = 0.56, 0.36, 0.70, 0.82, 0.50$  and  $0.57$  on June 09, 10, 11, 13, 14 and 15 2014 (Figs. 7-12) respectively.

Generally, from Figures 6-12 the IRI-Plas model  $NmF_2$  measurement has maximum positive percentage deviation  $4\%$  (Figs. 7 and 8) and minimum negative percentage deviation  $-7\%$  (Fig. 9). The model mostly underestimate from 18:00 UT to 05:00 UT and overestimate from 05:00 UT to 17:00 UT in most Figures. The maximum correlation coefficient is ( $R = 0.64$ , Fig. 10) and minimum value ( $R = 0.35$ , Fig. 11). The IRI-Plas model  $hmF_2$  measurement has maximum positive percentage deviation  $40\%$  (Figs. 6 and 7) and minimum negative percentage deviation  $-60\%$  (Fig. 12). The overestimation of the model is mostly from 05:00 UT to 15:00 UT in most Figures and underestimates mostly from 16:00 UT to 04:00 UT. The maximum correlation coefficient the model is ( $R = 0.11$ , Fig. 11) and minimum value ( $R = -0.49$ , Fig. 7). A negative correlation coefficient value demonstrates that the IRI-Plas 2017 model move in opposite directions, with a positive increase in the model data resulting in a decrease in the ionosonde data. The  $f_oF_2$  measurement of the IRI-Plas model has maximum positive percentage deviation  $45\%$  (Fig. 8) and minimum negative percentage deviation is around  $-50\%$ . The model mostly underestimate from 16:00 UT to 06:00 UT and overestimate from 07:00 UT to 15:00 UT in most Figures. The maximum correlation coefficient is ( $R = 0.82$ , Fig. 10) and minimum value ( $R = 0.36$ , Fig. 8).

The overall result, shows that the IRI-Plas 2017 model measurement of the  $f_oF_2$  values are in a good agreement with the ionosonde result than in  $hmF_2$  and  $NmF_2$ . This is in agreement with the study by Sezen et al (2018) and they found that the model values are closer to ionosonde results in  $f_oF_2$  than in  $hmF_2$ . Gordiyenko et al. (2019) found that the IRI-Plas model  $f_oF_2$  values are in a good agreement with the ionosonde measurement of the  $f_oF_2$  value during the diurnal variations, which is in agreement with the result of this study. And also the IRI-Plas 2017 model measurement of the  $NmF_2$  values are closer than in measurement of the  $hmF_2$  as shown from Figures 6-12.

## 4. Conclusion

The ionospheric parameters, such as total electron content (TEC), electron density profile (Ne), maximum electron density ( $NmF_2$ ), maximum ionization top of ionospheric layers ( $hmF_2$ ), critical layer frequency ( $f_oF_2$ ), electron and ion temperatures are modeled in different models, which are the most significant for trans-ionospheric radiowaves propagation, navigation and communications. This study has considered the determination of ionospheric parameters by using the IRI-Plas 2017 model performance comparison on months of the year 2014 with the ionosonde data measurement. In the comparison of the IRI-Plas 2017 model with the ionosonde data measurement the amount of error, the percent deviation and the correlation coefficient are used as the measure of the performance of the model. In most cases, the IRI-

Plas 2017 model overestimates with measurement values. The model has best correction with the measurement value in most days at around from 100 km to 200 km during the electron density measurement. The IRI-Plas 2017 model agrees well with the ionosonde electron density measurement from 100 km to 200 km altitude and mostly between from 0:00 UT to 06:00 UT and from 12:00 UT to 18:00 UT hours, whereas the model prejudices in other altitudes and hours with slightly less or more overestimation or underestimate in the ionosonde electron density measurement. The model has high percentage deviation value of electron density measurements mostly in between altitudes from 200 km to 450 km and during early nighttime and before midnight hours with values -21% and 8% for overestimation and underestimation respectively. The IRI-Plas 2017 model shows good correlation with the ionosonde electron density data after midnight and around midday, with less percentage deviation. The model has a large percentage deviation value for electron density observations at altitudes ranging from 200 km to 450 km, as well as throughout the early evening and before midnight. The IRI-Plas 2017 model results of NmF2, hmF2, and foF2 are primarily underestimates from ionosonde data at night (18:00 UT-06:00 UT) and overestimates during the day (06:00 UT-18:00 UT). The IRI-Plas 2017 model measurements of foF2 values agree better with ionosonde results than hmF2 and NmF2, and the model measurements of NmF2 values agree better than hmF2.

## Declarations

### Author Contribution

**Lake Endeshaw:** Conceptualization, methodology, validation, investigation, formal analysis, writing original draft, review and editing.

**Alene Seyoum:** Formal analysis, investigation, reviewing and editing.

### Funding

The authors of this study did not receive any internal and external funding. The organization and institution mentioned in the study have no role in the design and funding of the study.

### Declaration of Competing Interest

The authors declare that they have no known competing financial interests or personal relationships that could have appeared to influence the work reported in this paper.

### Data availability

The data used in this paper came from publicly available sources. The online IRI-Plas model is presented at the site, <http://www.ionolab.org/iriplasonline/>. The ionosonde observations can be found on the SPIDR website <http://spidr.ngdc.noaa.gov/spidr/>.

### Acknowledgments

We would like to acknowledge and thank the working groups of the IONOLAB Ionospheric Research Laboratory and Addis Ababa ionosonde station for the access of the IRI-Plas 2017 model ionosonde data respectively. The Online IRI-Plas can be accessed at [www.ionolab.org](http://www.ionolab.org). The ionosonde data is obtained from Addis Ababa ionosonde station.

## References

1. Adebisi SJ, Adimula IA, Oladipo OA, Joshua BW (2016) Assessment of IRI and IRI-Plas models over the African equatorial and low-latitude region. *J. Geophys. Res. Space Phys.* 121:7287-7300. <https://doi.org/10.1002/2016JA022697>.
2. Alçay S, Oztan G, Selvi HZ (2017) Comparison of IRI-PLAS and IRI-2012 model predictions with GPS-TEC measurements in different latitude regions. *Ann. Geophys.* 60(5)
3. Arikan F, Sezen U, Gulyaeva T, Cilibas O (2015) Online, automatic, ionospheric maps: IRI-PLAS-MAP. *Adv. Space Res.* 55(8): 2106-2113
4. Cherniak I, Zakharenkova I (2016) NeQuick and IRI-Plas model performance on topside electron content representation: spaceborne GPS measurements, *Radio Sci.* 51 (6) ,752-766.
5. Davies K (1990) Ionospheric radio. Issue 31 of IEE electromagnetic waves series. Peter Peregrinus Ltd., IEE, London.
6. Endeshaw L (2020) Testing and validating IRI-2016 model over Ethiopian ionosphere. *Astrophys Space Sci* **365**, 49, <https://doi.org/10.1007/s10509-020-03761-1>
7. Ezquer RG, Scidá LA, Orué YM, Nava B, Cabrera MA, Brunini C (2018) NeQuick 2 and IRI Plas VTEC predictions for low latitude and South American sector. *Adv. Space Res.* 61(7), 1803-1818
8. Gordiyenko GI, Maltseva OA, Arikan F, Yakovets AF (2019) An evaluation of the IRI-Plas-TEC for winter anomaly along the mid-latitude sector based on GIM-TEC and foF2 values. *Adv. Space Res.* 64 2046-2063 <https://doi.org/10.1016/j.asr.2019.04.014>
9. Gordiyenko GI, Maltseva OA, Arikan F, Yakovets, A.F., 2018. The performance of the IRI-Plas model as compared with Alouette II and GIM-TEC data over the midlatitude station Alma-Ata. *J. Atmos. Solar. Terr. Phys.* 179, 504-516. <https://doi.org/10.1016/j.jastp.2018.08.007>.
10. Gulyaeva TL, Huang X, Reinisch B (2002a) Ionosphere-Plasmasphere Model Software for ISO. *Acta Geod. Geoph. Hung* 37(2-3), 143-152
11. Gulyaeva TL, Huang X, Reinisch B (2002b) Plasmaspheric extension of topside electron density profiles. *Adv. Space Res.* 29:825-831
12. Gulyaeva TL, Arikan F, Hernandez-Pajares M, Stanislawski I (2013) GIM-TEC adaptive ionospheric weather assessment and forecast system. *J. Atmos. Sol. Terr. Phys.* 102, 329-340 <https://doi.org/10.1016/j.jastp.2013.06.011>
13. Hargreaves J (1992) *The Solar-Terrestrial Environment*, Cambridge University Press, New York, US
14. Kutiev I, Tsagouri I, Perrone L, Pancheva D, Mukhtarov P, Mikhailov A, Lastovicka J, Jakowski J, Buresova D, Blanch E, Andonov B, Altadill D, Magdaleno S, Parisi M, Torta JM (2013) Solar activity

impact on the Earth's upper atmosphere. *J Space Weather Space Clim* 3:A06.

<https://doi.org/10.1051/SWSC/2013028>

15. Maltseva OA, Zhibankov A, Mozhaeva NS (2013) Advantages of the new model of IRI (IRI-Plas) to simulate the ionospheric electron density: case of the European area. *Adv. Radio. Sci.* 11 (2) 307-311
16. Maltseva OA, Mozhaeva NS, Nikitenko TV (2015) Comparative analysis of two new empirical models IRI-Plas and NGM (the Neustrelitz Global Model). *Adv. Space Res.* 55 (8) 2086-2098
17. Okoh DS, Onwuneme G, Seemala SH, Jin B, Rabiou B, Nava J, Uwamahoro (2018) Assessment of the NeQuick-2 and IRI-Plas 2017 models using global and long-term GNSS measurements. *J. Atmos. Sol. Terr. Phys.* 70 1-10
18. Panda SK, Gedam SS, Rajaram G (2015) Study of Ionospheric TEC from GPS observations and comparisons with IRI and SPIM model predictions in the low latitude anomaly Indian subcontinental region. *Adv. Space Res.* 55 (8) 1948-1964
19. Rawer K (2013) *Wave propagation in the ionosphere, developments in electromagnetic theory and applications.* Springer Science and Business Media, New York
20. Reinisch BW, Huang X (2001) Deducing topside profiles and total electron content from bottomside ionograms. *Adv Space Res* 27(1):23-30
21. Sezen U, Gulyaeva TL, Feza Arikani (2018) Online computation of International Reference Ionosphere Extended to Plasmasphere (IRI-Plas) model for space weather. *Geodesy and Geodynamics* 9 347-357, <https://doi.org/10.1016/j.geog.2018.06.004>
22. Seyoum A, Gopalswamy N, Nigussie M, Mezgebe N (2019) The impact of CMEs on the critical frequency of F2-layer ionosphere (foF2). *Proceedings of the International Astronomical Union*, 15(S356), 400-402. <https://doi.org/10.1017/S1743921320003579>
23. Titheridge JE (1985) *Ionogram Analysis with the Generalised Program POLAN.* Report UAG-93, University of Auckland, New Zealand.
24. Zakharenkova I, Cherniak IV, Krankowski A, Shagimuratov I (2015) Vertical TEC representation by IRI 2012 and IRI Plas models for European midlatitudes. *Adv. Space Res.* 55(8), 2070-2076
25. Zhang ML, Liu L, Wan W, Ning B (2017) Comparison of the observed topside ionospheric and plasmaspheric electron content derived from the COSMIC podTEC measurements with the IRI-Plas model results. *Adv. Space Res.* 60, 222-227.

## Figures

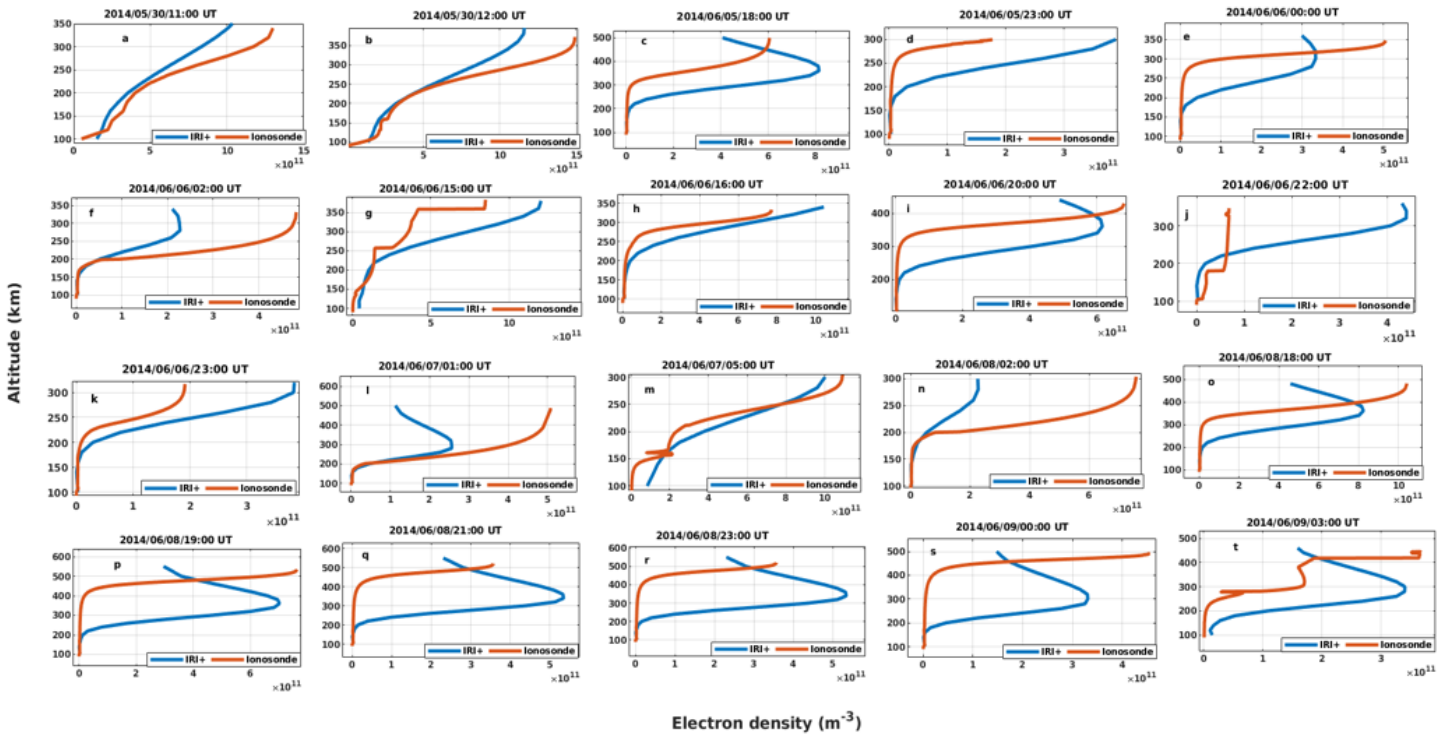
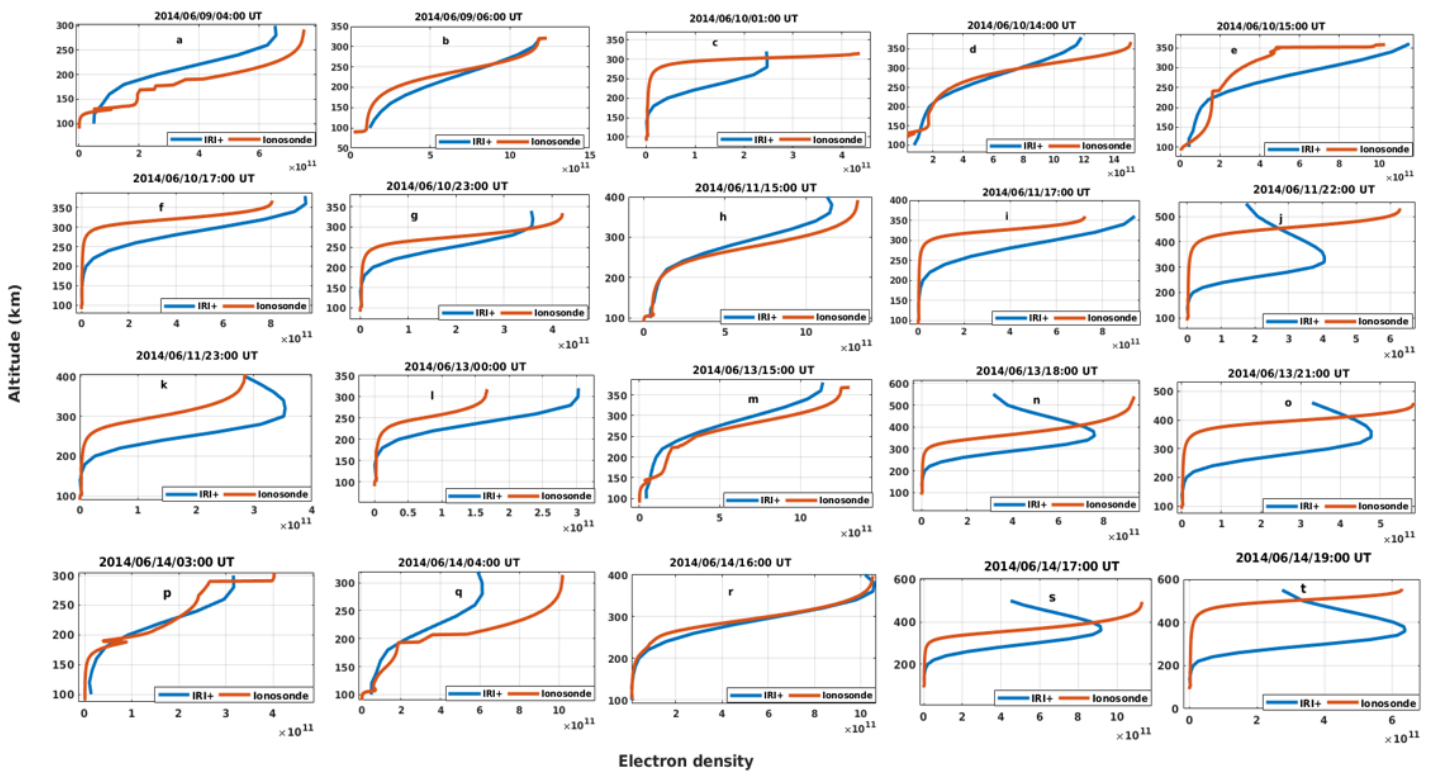


Figure 1

Altitudinal variations of the electron density profile values obtained from ionosonde and IRI-Plas 2017 model on days of May and June 2014 months in different hours.



**Figure 2**

Altitudinal variations of the electron density profile values obtained from ionosonde and IRI-Plas 2017 model on days of June 2014 in different hours.

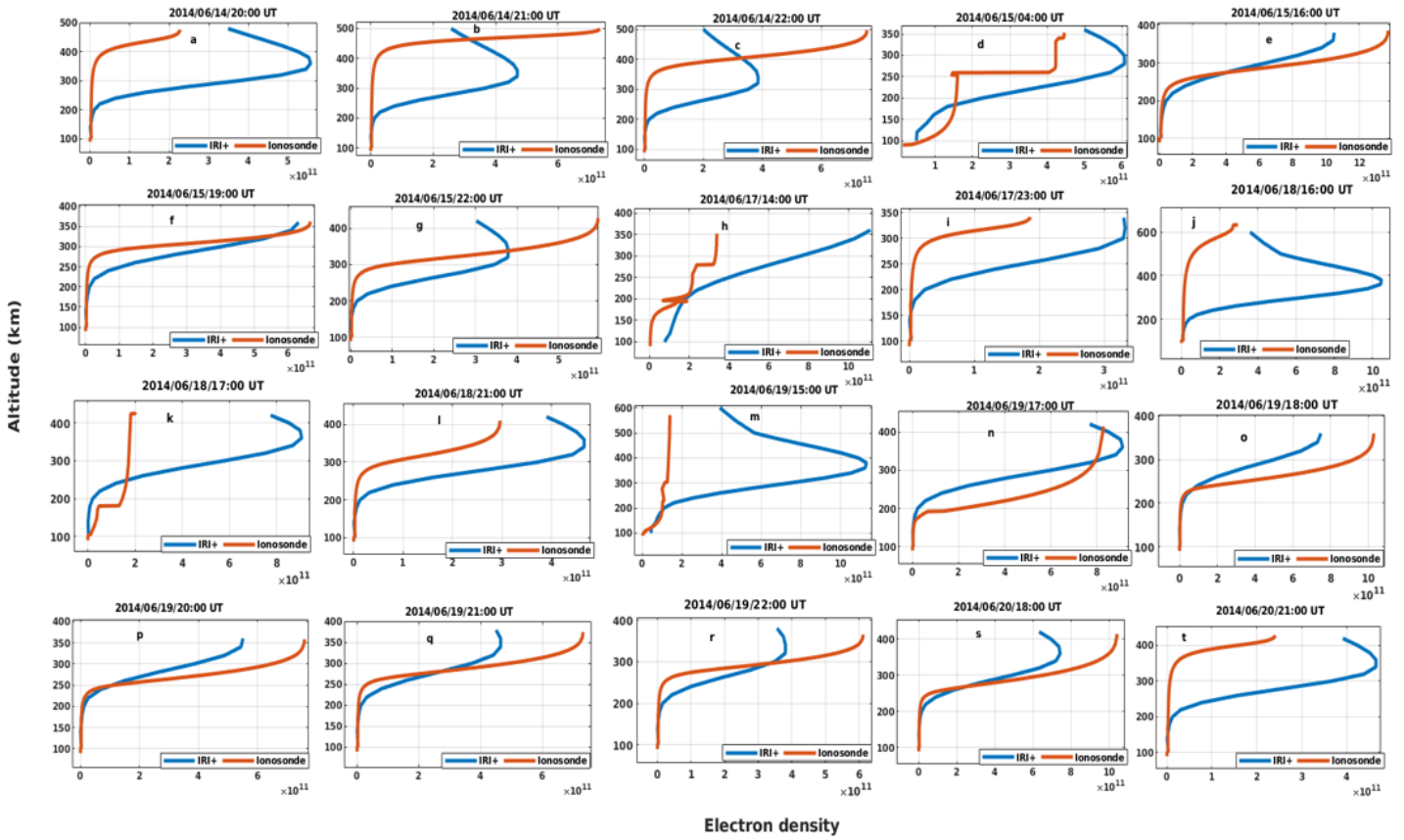


**Figure 3**

Altitudinal variations of the electron density profile values obtained from ionosonde and IRI-Plas 2017 model on different hours of days June 2014.

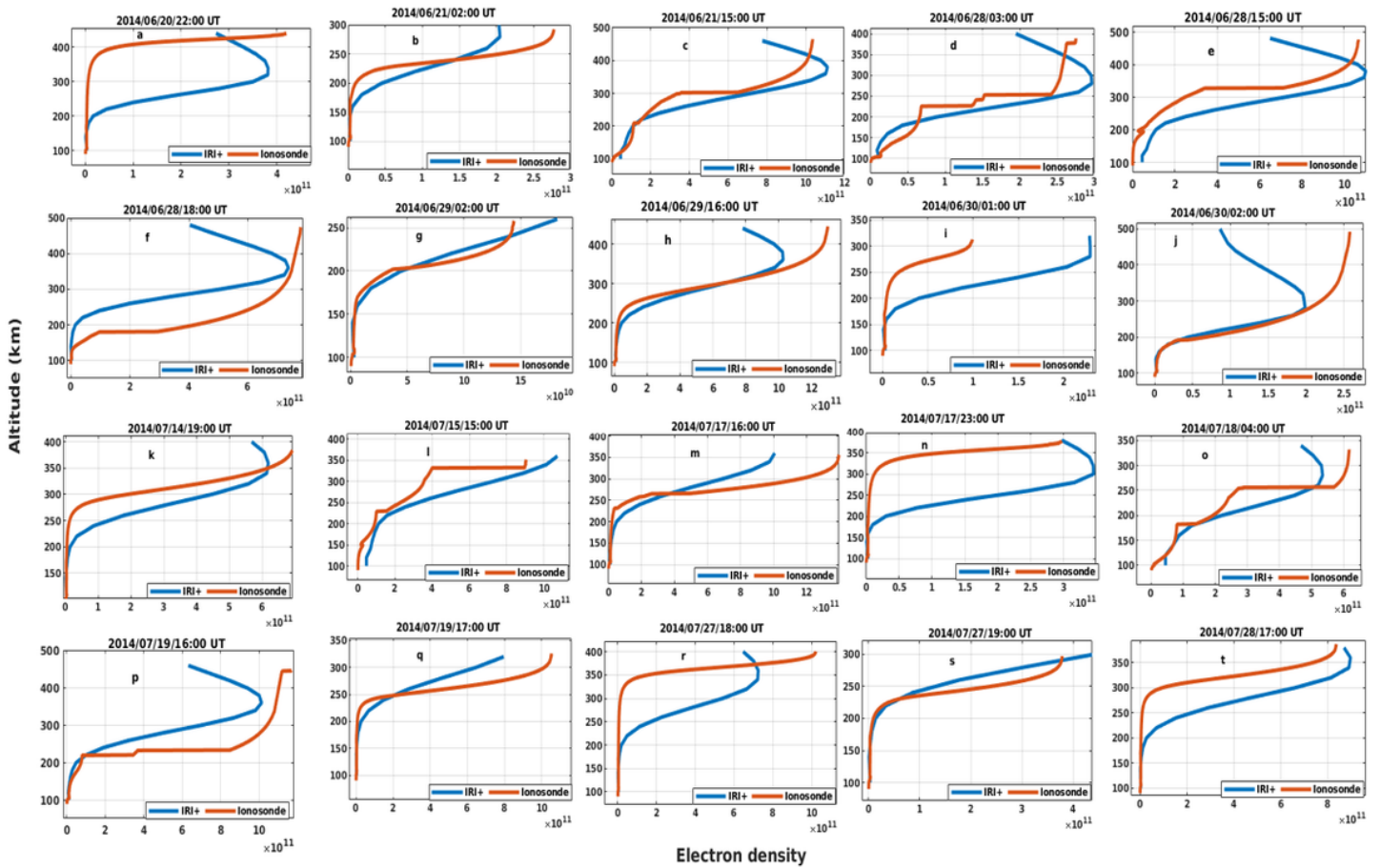


**Figure 4**

Altitudinal variations of the electron density profile values obtained from ionosonde and IRI-Plas 2017 model on days of June and July 2014 months in different hours.

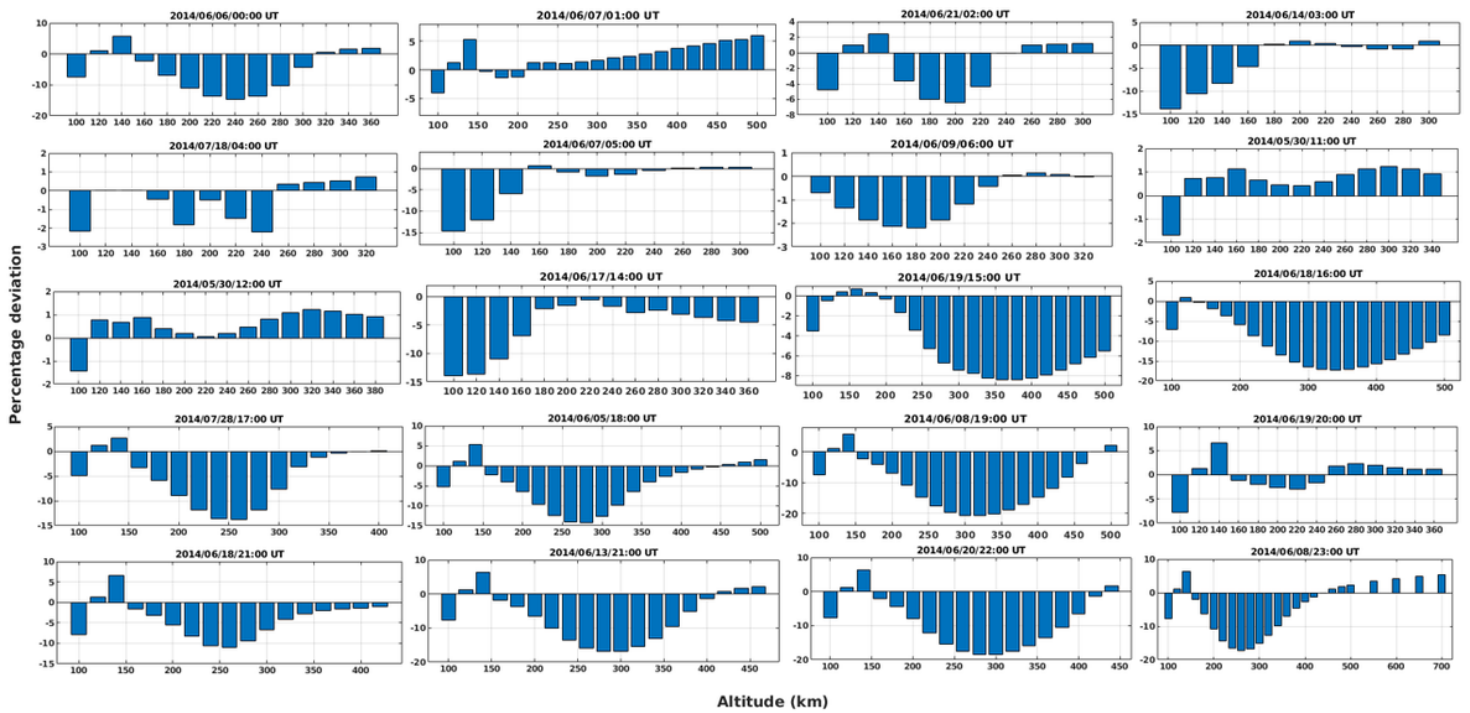


Figure 5

Hourly percentage deviation values of the IRI-Plas 2017 model from ionosonde electron density measurements in different days of months (May, June and July) for different hours

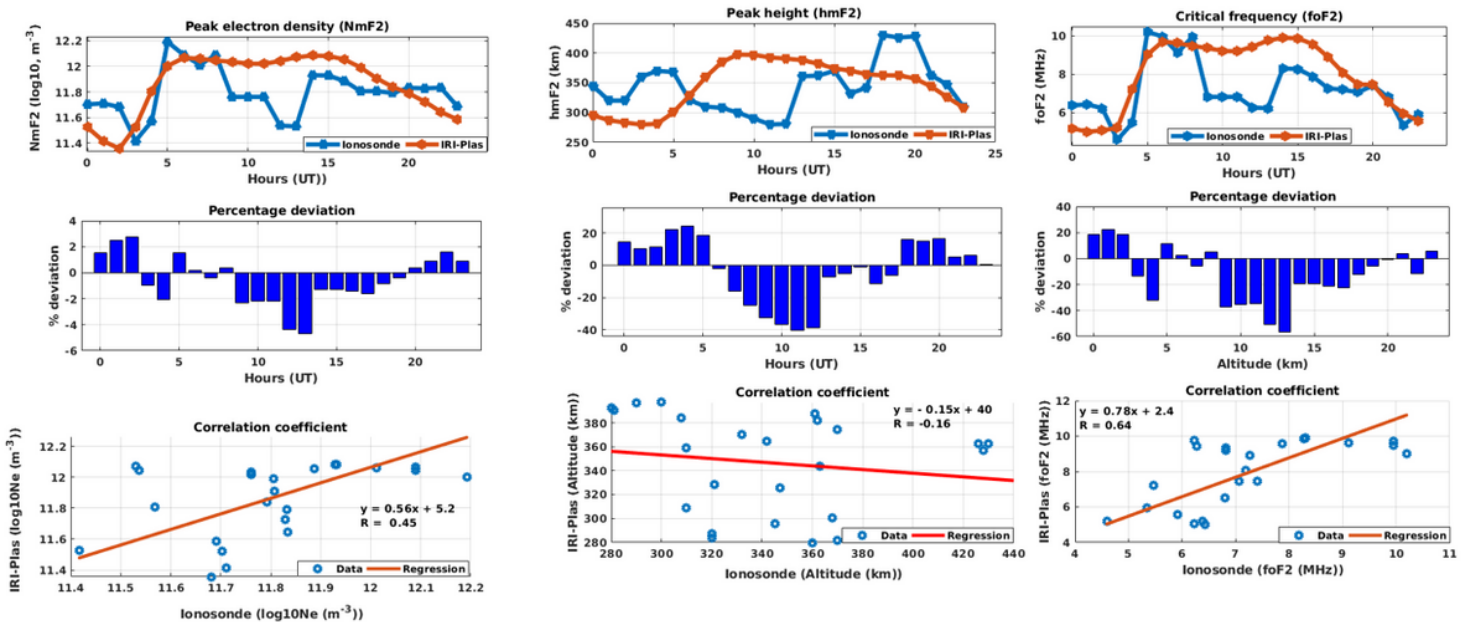


Figure 6

Hourly variability of peak electron density, NmF2 (left side), peak height, hmF2 (middle) and critical frequencies, foF2 (right side) with their values of percentage deviation and correlation coefficients (R) of the IRI-Plas 2017 model from ionosonde measurements on June 06 2014

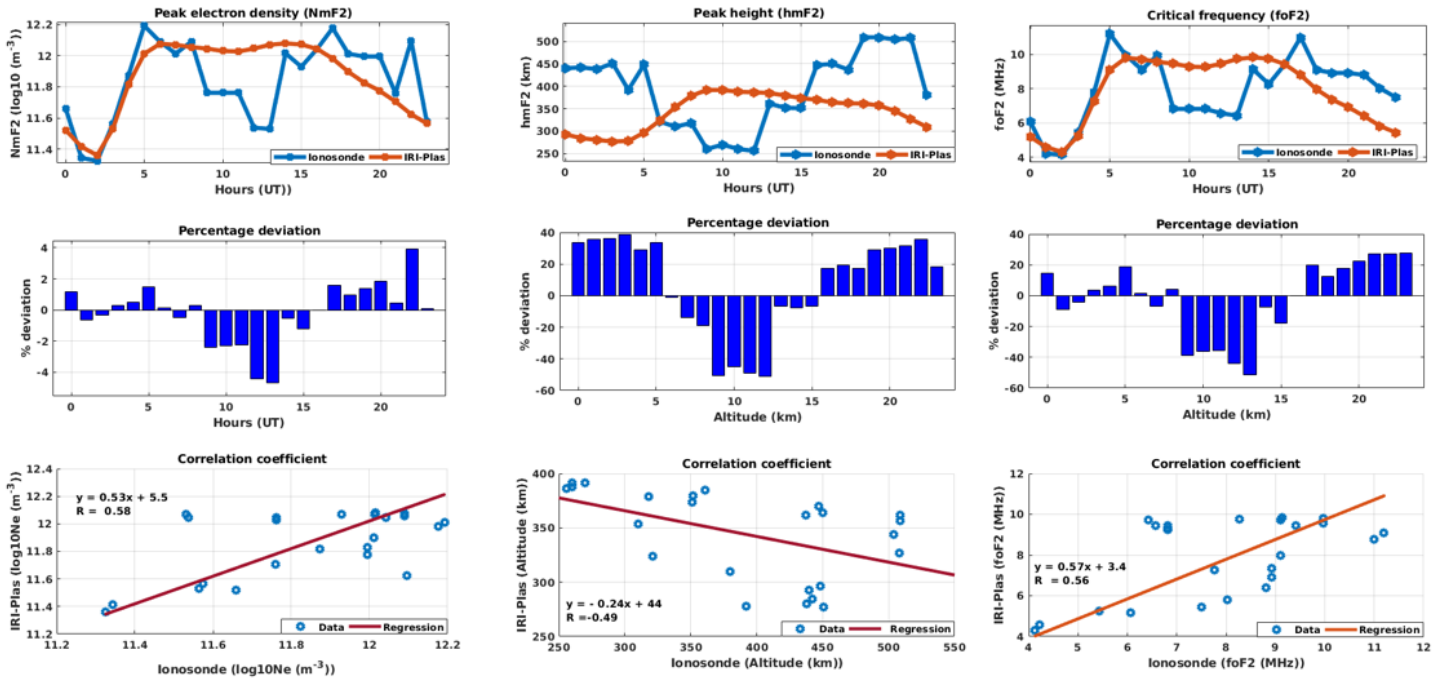


Figure 7

Hourly variability of peak electron density, NmF2 (left side), peak height, hmF2 (middle) and critical frequencies, foF2 (right side) with their values of percentage deviation and correlation coefficients (R) of the IRI-Plas 2017 model from ionosonde measurements on June 09 2014

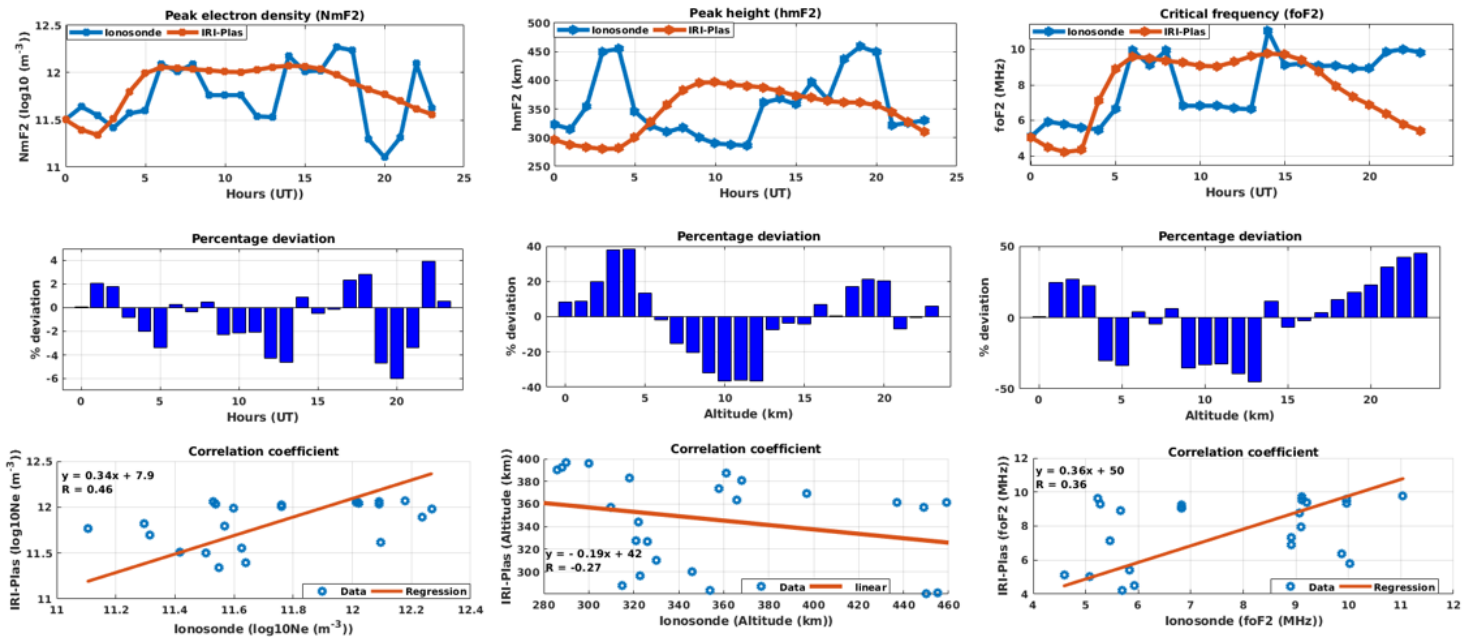


Figure 8

Hourly variability of peak electron density, NmF2 (left side), peak height, hmF2 (middle) and critical frequencies, foF2 (right side) with their values of percentage deviation and correlation coefficients (R) of the IRI-Plas 2017 model from ionosonde measurements on June 10 2014

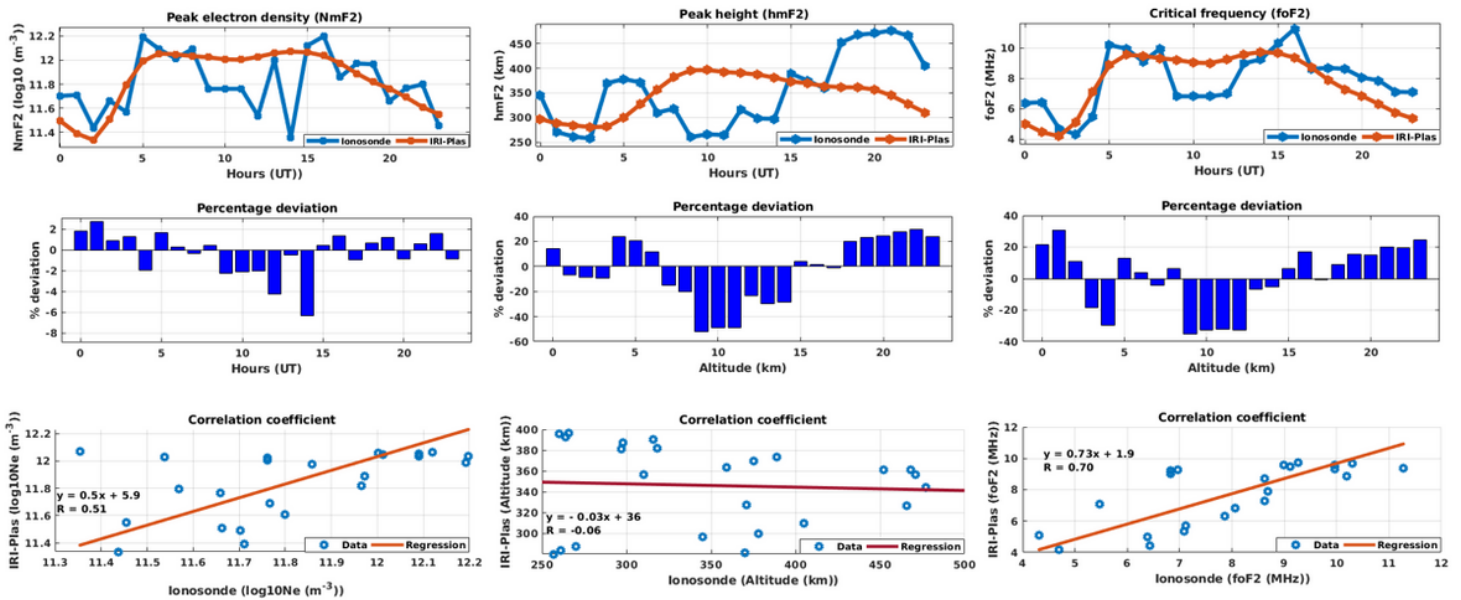


Figure 9

Hourly variability of peak electron density, NmF2 (left side), peak height, hmF2 (middle) and critical frequencies, foF2 (right side) with their values of percentage deviation and correlation coefficients (R) of the IRI-Plas 2017 model from ionosonde measurements on June 11 2014

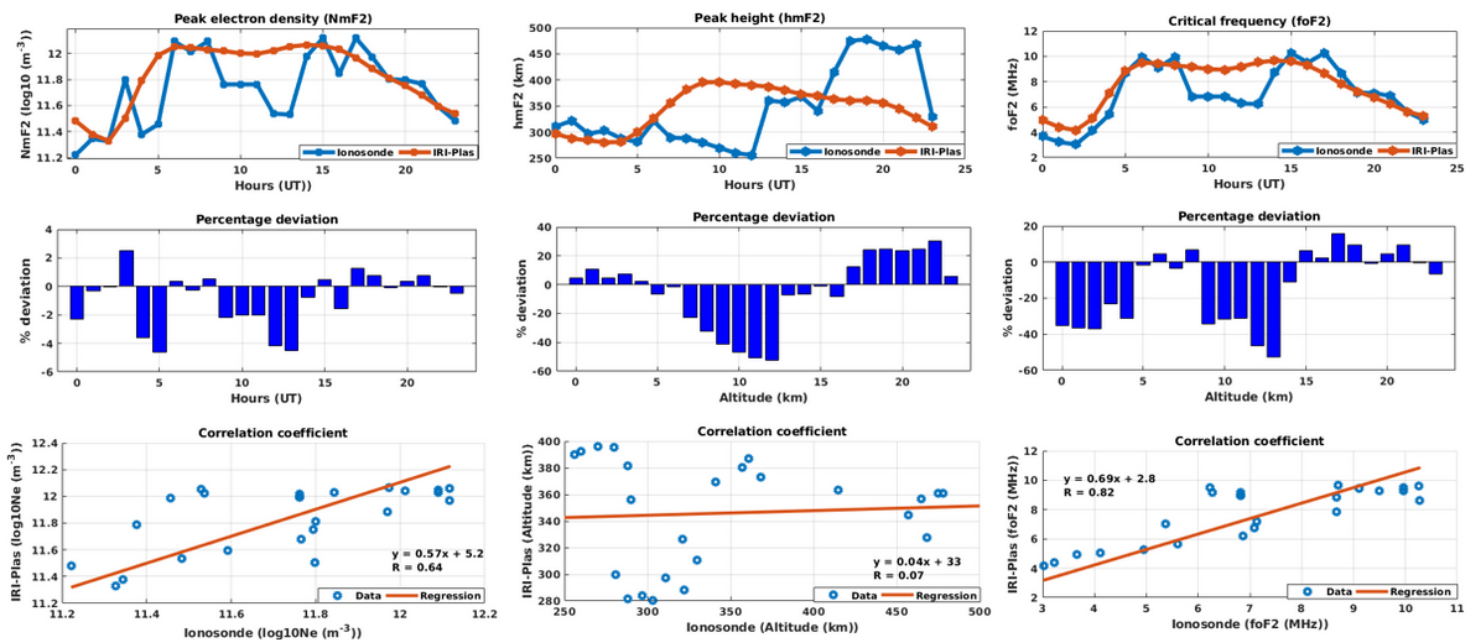


Figure 10

Hourly variability of peak electron density, NmF2 (left side), peak height, hmF2 (middle) and critical frequencies, foF2 (right side) with their values of percentage deviation (bar graph) and correlation coefficients (R) of the IRI-Plas 2017 model from ionosonde measurements on June 13 2014.

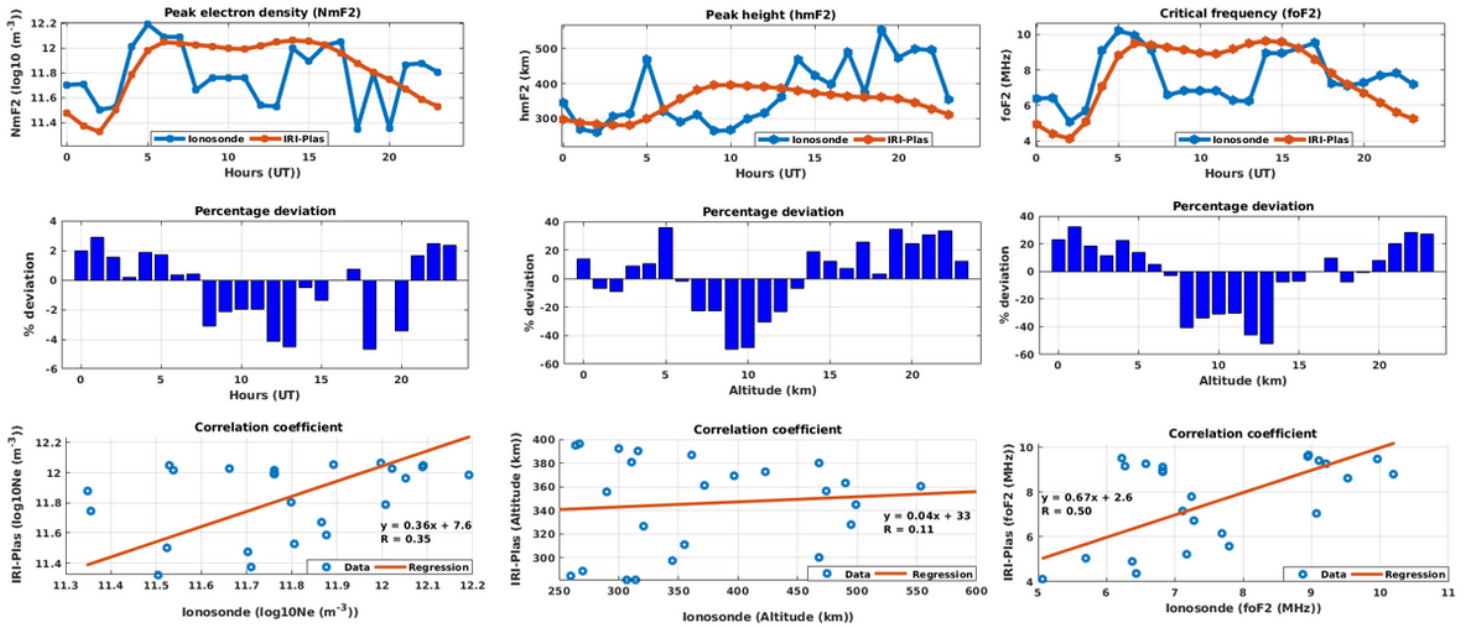


Figure 11

Hourly variability of peak electron density, NmF2 (left side), peak height, hmF2 (middle) and critical frequencies, foF2 (right side) with their values of percentage deviation and correlation coefficients (R) of the IRI-Plas 2017 model from ionosonde measurements on June 14 2014

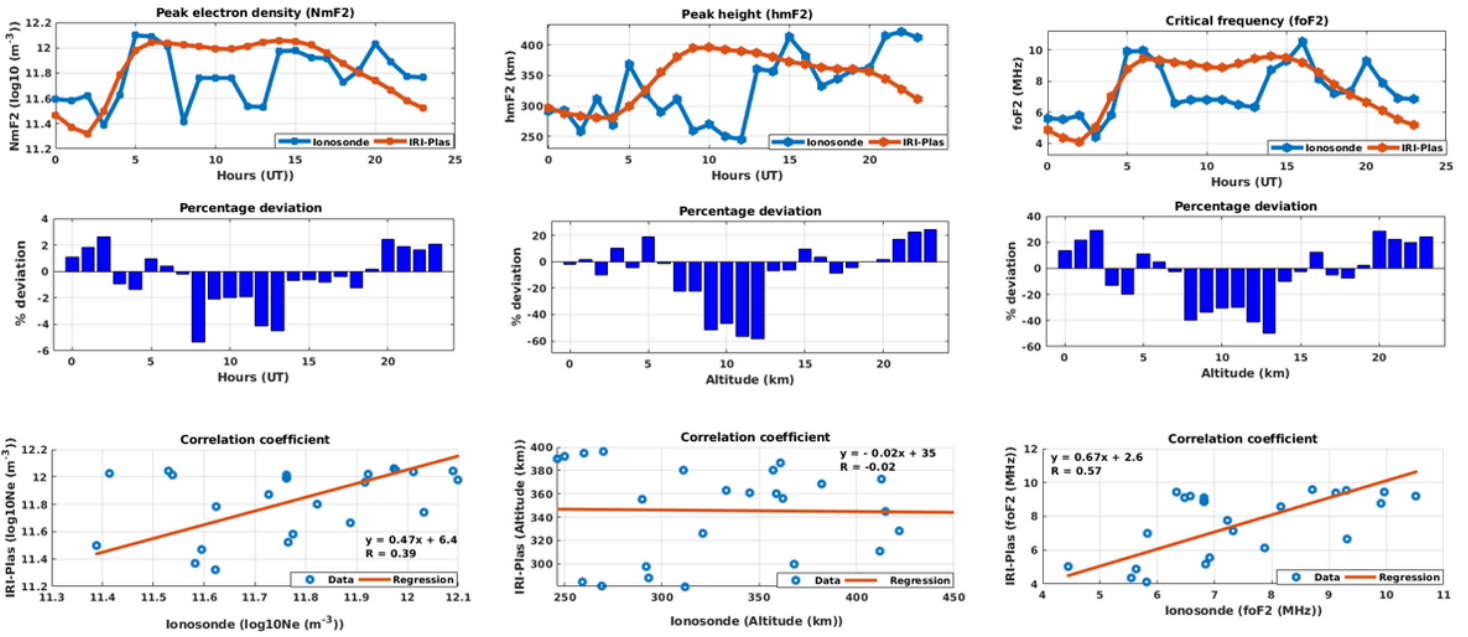


Figure 12

Hourly variability of peak electron density, NmF2 (left side), peak height, hmF2 (middle) and critical frequencies, foF2 (right side) with their values of percentage deviation and correlation coefficients (R) of the IRI-Plas 2017 model from ionosonde measurements on June 15 2014

## Supplementary Files

This is a list of supplementary files associated with this preprint. Click to download.

- [Abstract.png](#)